Electronic Supplementary Information

for

Twisted terrylene dyes: synthesis and application in organic solar cells

Jiajing Feng,[ab] Ningning Liang,[ab] Wei Jiang,*[a] Dong Meng,[ab] Rui Xin,[c] Bowei Xu,[a] Jianqi Zhang,[d] Zhixiang Wei,[d] Jianhui Hou[a] and Zhaohui Wang*[a]

a. Beijing National Laboratory for Molecular Science, Key Laboratory of Organic Solids, CAS Research/Education Center for Excellence in Molecular Sciences, Institute of Chemistry, Chinese Academy of Sciences, Beijing 100190, P. R. China
b. University of Chinese Academy of Sciences, Beijing 100049, P. R. China
c. State Key Laboratory of Chemical Resourse Engineering, Beijing University of Chemical Technology, Beijing 100029, China
d. National Center for Nanoscience and Technology, Chinese Academy of Sciences, Beijing, 100190, China
**Email: jiangwei@iccas.ac.cn, wangzhaohui@iccas.ac.cn*

Table of contents

1. Materials and Methods

Materials. All chemicals and solvents were purchased from commercial suppliers and used without further purification unless otherwise specified.

Characterizations of compounds. ^{1}H NMR and ^{13}C NMR spectra were obtained in deuterated solvents on a Bruker ADVANCE 400 NMR or a Bruker ADVANCE 500 NMR Spectrometer. Chemical shifts are expressed in ppm using the residual protonated solvent as an internal standard. The signals have been named as follows: s (singlet), d (doublet), t (triplet), q (quartet), m (multiplets) and br (broad). High resolution mass spectra (HRMS) were determined on IonSpec 4.7 Tesla Fourier Transform Mass Spectrometer.

Optical characterizations. UV-vis absorption spectra were measured with Hitachi (Model U-3010) UV-vis spectrophotometer in a 1 cm quartz cell.

Electrochemical characterizations. Cyclic voltammograms (CVs) were recorded on a Zahner IM6e electrochemical workstation, with glassy carbon discs as the working electrode, Pt wire as the counter electrode, Ag/AgCl electrode as the reference electrode at a scanning rate of 100 mV/s. 0.1 M tetrabutylammoniumhexafluorophosphate (Bu_4NPF_6) dissolved in CH_2Cl_2 or CH_3CN (HPLC grade) was used as the supporting electrolyte, which was calibrated by the redox couple of ferrocene/ferroncenium (Fc/Fc^+).

Thermal characterizations. Thermogravimetric analysis (TGA) was measured on a PE TGA-7 instrument with a dry nitrogen flow. Temperature was programmed from room temperature and ramped at 10 °C/min to 550 °C. Differential scanning calorimetry (DSC) analyses were measured on TA DSC 2010 instrument under a dry nitrogen flow, heating from 0 °C to 330 °C and cooling from 330 °C to 0 °C at a rate of 10 °C min^{-1}.

Morphological characterizations. Atomic force microscopy (AFM) measurements were carried out with a Nanoscope IIIa instrument (Digital Instruments).

Carrier mobility measurements. Carrier mobility was determined by space charge limit current (SCLC) method. The hole and electron mobility were measured with the device structure of ITO/PEDOT:PSS/PBDT-TS1:acceptors/Au and ITO/ZnO/PBDT-TS1:acceptors/Al, respectively. The mobility was described by the equation:

$$J = 9\varepsilon_0\varepsilon_r\mu_e V^2/8L^3,$$

$$J \cong (\frac{9}{8})\varepsilon_r\varepsilon_0\mu_h V^2 exp(0.89\sqrt{\frac{V}{E_0 L}})/L^3,$$

where J is the current density, L is the film thickness of the active layer, μ_h is the hole mobility, μ_e is the electron mobility, ε_r is the relative dielectric constant of the transport medium, and ε_0 is the permittivity of free space. $V = V_{app} - V_{bi}$, where V_{app} is the applied voltage, V_{bi} is the offset voltage (V_{bi} is 0.2 V here).[1]

Grazing incidence wide angle X-ray scattering (GIWAXS) measurements. GIWAXS measurements were carried out in a Xenocs-SAXS/WAXS system with X-ray wavelength of 1.5418 Å. The samples were irradiated at a fixed angle of 0.2. The films were made on Si wafer substrates under the same preparation conditions for solar cells.

2. Synthesis and characterization of TDI2 and BTDI3

The starting material **TDI** was synthesized according to literature procedures.[2]

***N*,*N*'-bis-(1-heptyloctyl)-1-bromoterrylene-3,4,11,12-tetracarboxdiimide (1):** a solution of *N*,*N*'-bis-(1-heptyloctyl)-terrylene-3,4,11,12-tetracarboxdiimide (1 g, 1.07 mmol) in CH_2Cl_2 (200 mL) was cooled in ice-water bath. Then a diluted solution of bromine (5 mL) in CH_2Cl_2 (20 mL) was added drop by drop over a period of 30 min. The reaction mixture was stirred at 0 ^oC for additional 30 min. Next, the excess of bromine was quenched with saturated sodium sulfite solution. The organic layer was separated, dried over $MgSO_4$, and purified by silica gel column chromatography (petroleum ether/CH_2Cl_2, 3:2 v/v) to give **1** as a blue solid (660 mg, 60.8%).

^1H NMR (500 MHz, $CDCl_2CDCl_2$, 373K): δ = 9.74-9.72 (d, J = 8.6 Hz, 1H), 8.90 (s, 1H), 8.65-8.61 (m, 3H), 8.59-8.58 (m, 2H), 8.55-8.52 (m, 3H), 8.50-8.48 (d, J = 8.1 Hz, 1H), 5.19-5.17 (m, 2H), 2.27-2.25 (m, 4H), 1.94-1.91 (m, 4H), 1.37-1.28 (m, 40H), 0.87-0.86 (m, 12H); ^{13}C NMR (100 MHz, $CDCl_2CDCl_2$): δ = 164.45, 163.57, 162.56, 139.19, 138.55, 135.06, 134.73, 134.41, 134.03, 131.46, 131.16, 130.82, 130.54, 129.67, 129.34, 128.96, 128.76, 128.09, 127.96, 127.51, 125.49, 123.78, 122.90, 122.45, 122.15, 121.96, 121.63, 121.44, 118.83, 54.94, 54.68, 32.43, 31.94, 29.68, 29.38, 29.37, 27.25, 27.18, 22.76, 14.28; HRMS (MALDI, 100%): calcd (%) for $C_{64}H_{73}BrN_2O_4$: 1012.4759; found, 1012.4759.

TDI2: compound **1** (400 mg, 0.394 mmol), zinc powder (128 mg, 1.97 mmol) and tris(dibenzylideneacetone)dipalladium(0) (36 mg, 0.039 mmol) were added into a two necked flask under an argon atmosphere. Then anhydrous *N*,*N*'-Dimethylformamide (10 mL) was added by injection. The mixture was heated to 60 ^oC with vigorous stirring for 1 h. After cooling down, the mixture was poured into 2 M hydrochloric acid solution, and the precipitate was collected by vacuum filtration, washed with water, dried, and purified by column chromatography on silica gel (petroleum ether /CH_2Cl_2, 1:1 v/v) to afford **TDI2** as a dark blue solid (191 mg, 51.9%).

^1H NMR (500 MHz, $CDCl_2CDCl_2$, 373 K): δ = 8.77-8.75 (d, J = 8.15 Hz, 2H), 8.68-8.65 (m, 4H), 8.57-8.51 (m, 6H), 8.46-8.45 (d, J = 8.1 Hz, 2H), 8.42 (s, 2H), 8.39-8.38 (d, J = 8.15 Hz, 2H), 8.20-8.18 (d, J = 8.2 Hz, 2H), 8.07-8.05 (d, J = 8.65 Hz, 2H), 5.18-5.08 (m, 4H), 2.26-2.14 (m, 8H), 1.92-1.81 (m, 8H) , 1.36-1.19 (m, 80H) , 0.85-0.77 (m, 24H); ^{13}C NMR (125 MHz,

$CDCl_2CDCl_2$, 373 K): δ = 164.09, 163.73, 140.43, 135.79, 135.33, 135.05, 133.86, 131.38, 130.93, 130.73, 129.88, 129.63, 129.05, 128.67, 128.45, 125.95, 124.49, 124.26, 123.53, 122.56, 122.25, 121.60, 54.91, 54.78, 32.57, 32.48, 31.72, 31.67, 29.45, 29.39, 29.36, 29.08, 29.02, 27.02, 26.95, 22.46, 22.41, 13.85; HRMS (MALDI , 100%): calcd (%) for $C_{128}H_{146}N_4O_8$: 1867.1146; found, 1867.1143.

BTDI3: a Schlenk flash was charged with compound **1** (300 mg, 0.296 mmol), 1,3,5-benzenetriboronic acid tris(pinacol) ester (42 mg, 0.092 mmol) and tetrakis(triphenylphosphine)palladium(0) (21 mg, 0.018 mmol) under argon. Then tetrahydrofuran (8 mL) and 2 M anhydrous potassium carbonate solution (4 mL) was adding by injection, and the reaction mixture was heated to 90 ºC for 12 h. After cooling down and removal of the solvent under vacuum, the residue was purified by column chromatography on silica gel (petroleum ether /CH_2Cl_2, 1:1 v/v) to yield blue solid **BTDI3** (180 mg, 68.2%).

^{1}H NMR (500 MHz, $CDCl_2CDCl_2$, 373 K): δ = 8.71-8.53 (m, 33H), 8.02 (s, 3H), 5.15 (br, 3H), 4.97 (br, 3H), 2.22 (br, 8H), 1.90 (br, 12H), 1.67 (br, 8H), 1.28-1.16 (m, 116H), 0.86-0.80 (m, 36H); ^{13}C NMR (125 MHz, $CDCl_2CDCl_2$, 373 K): δ = 164.13, 147.72, 137.93, 135.83, 135.61, 135.45, 135.24, 133.52, 131.65, 131.51, 130.96, 130.22, 129.77, 129.30, 128.94, 128.88, 127.81, 126.20, 124.39, 124.26, 122.75, 122.14, 121.62, 54.71, 32.60, 32.43, 31.76, 31.70, 29.49, 29.37, 29.09, 29.04, 27.05, 26.90, 22.48, 22.45, 13.87; HRMS (MALDI, 100%): calcd (%) for $C_{198}H_{222}N_6O_{12}$: 2875.6951; found, 2875.6991.

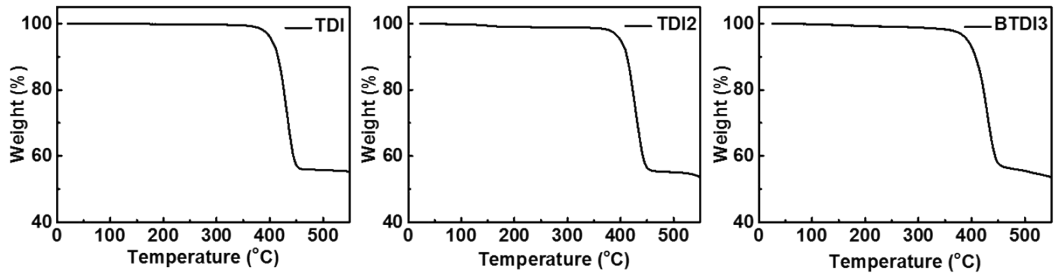

Fig. S1 The TGA plots of the three molecules.

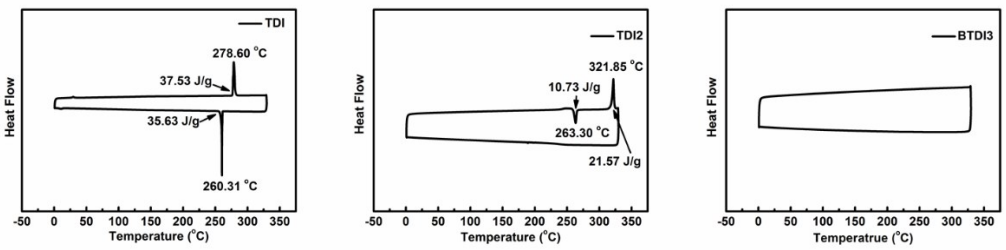

Fig. S2 The DSC plots of the three molecules.

Table S1 The photophysical properties of **TDI**, **TDI2** and **BTDI3**

Compounds	λ_{max}^{sol} [nm][a]	ε [$M^{-1}cm^{-1}$][a]	λ_{max}^{film} [nm][b]	ΔE^{opt} (sol.) [eV][c]	ΔE^{opt} (film.) [eV][d]
TDI	652	165300	669	1.82	1.69
TDI2	624	120400	632	1.65	1.55
BTDI3	658	249500	669	1.76	1.68

[a] Measured in dilute $CHCl_3$ solution (1.0×10^{-5} M). [b] Measured in spin-coating film from $CHCl_3$ solution. [cd] Calculated by the onset of absorption in $CHCl_3$ solution and in films according to E_g (eV) = (1240/λ_{onset}).

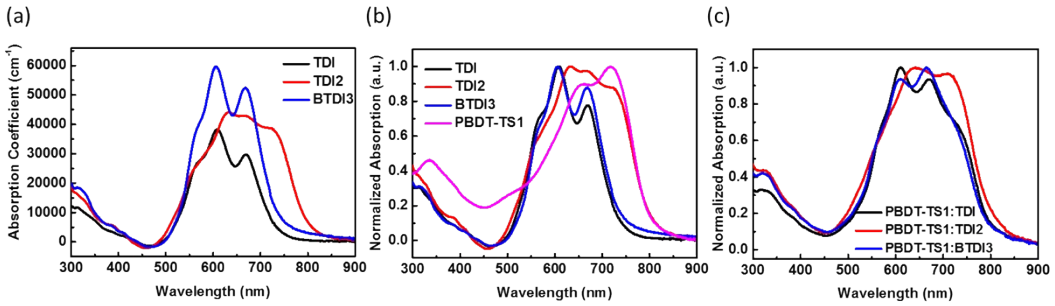

Fig. S3 UV-vis absorption spectra of (a) neat **TDI**, **TDI2**, **BTDI3** films, (b) neat **TDI**, **TDI2**, **BTDI3** and PBDT-TS1 films and (c) blend films.

Table S2 Electrochemical properties of **TDI**, **TDI2** and **BTDI3**

	E_{1r} [V][a]	E_{2r} [V][a]	E_{1o} [V][a]	E_{2o} [V][a]	HOMO/LUMO (sol.)[eV][a]	ΔE^{cv} (sol.) [eV][a]	HOMO/LUMO (film)[eV][b]	ΔE^{cv} (film) [eV][b]
TDI	-1.12	—	0.71	—	-5.49/-3.89	1.60	-5.55/-3.79	1.76
TDI2	-1.00	-1.19	0.70	0.78	-5.50/-3.99	1.51	-5.67/-3.94	1.73
BTDI3	-1.01	—	0.71	—	-5.54/-3.86	1.68	-5.71/-3.88	1.83

[a] In CH_2Cl_2 solution vs. Fc/Fc^+, LUMO (eV) estimated by the onset of the reduction peaks and calculated according to E_{LUMO} = -(4.8 + E_{onset}^{re}) eV, HOMO (eV) calculated according to E_{HOMO} = -(4.8 + E_{onset}^{ox}) eV. [b] in film vs. Fc/Fc^+, LUMO (eV) estimated by the onset of the reduction peaks and calculated according to E_{LUMO} = -(4.8 + E_{onset}^{re}) eV, HOMO (eV) calculated according to E_{HOMO} = -(4.8 + E_{onset}^{ox}) eV.

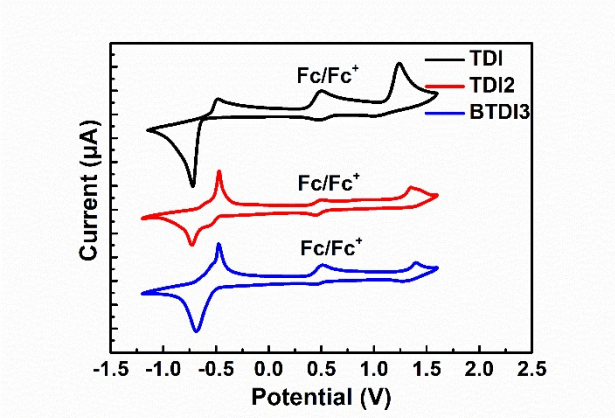

Fig. S4 Cyclic voltammograms of the three molecules in films.

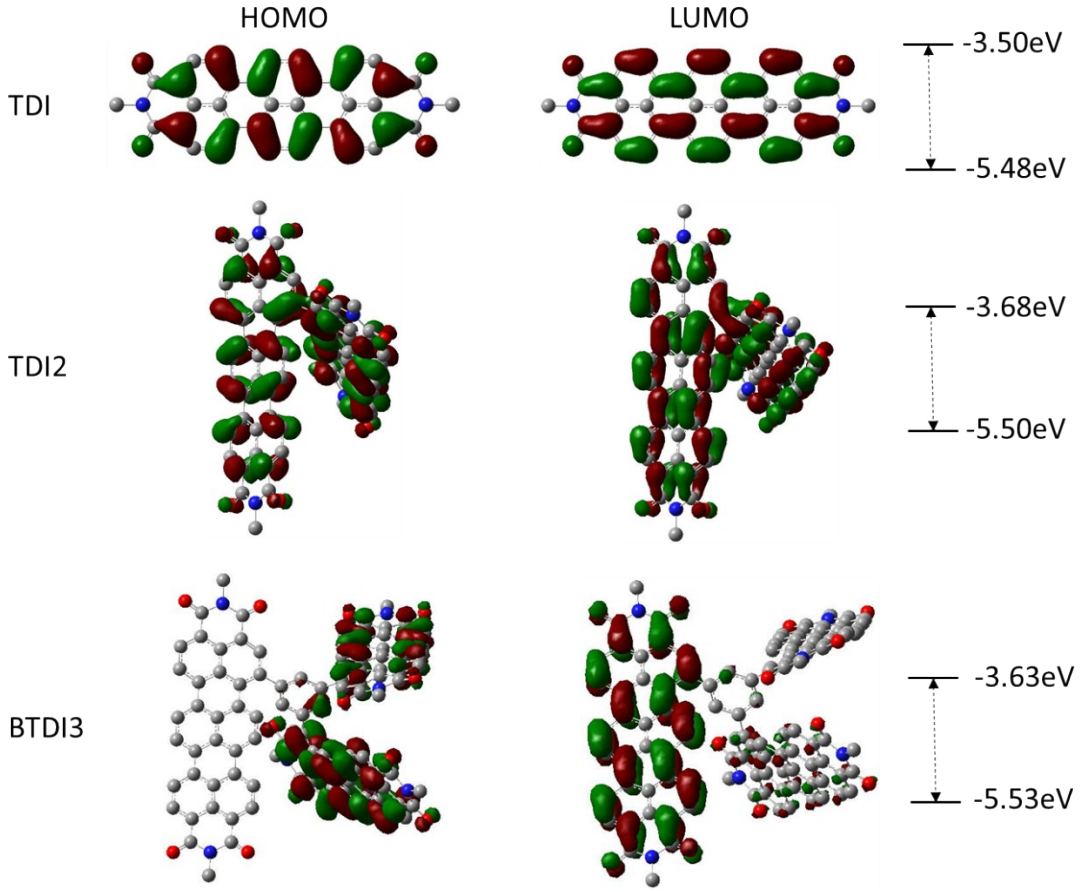

Fig. S5 Optimized geometries, HOMO and LUMO of **TDI**, **TDI2** and **BTDI3** by DFT at the B3LYP/6-31G(d) level.[3]

3. OPV Device Fabrication and Characterization

The ZnO solution, which was used to make the cathode buffer layers, was synthesized according to the previous literature.[4] ITO(15 Ω/sq) was cleaned ultrasonically with detergent, deionized (DI) water, acetone and isopropanol, respectively. The dried ITO-glass was treated with UV-ozone for 20 minutes and then it was spin-coated the ZnO solution on the surface using 4000 rpm for 30 seconds. Then the PBDT-TS1:acceptor blend solution was spin-coated on the ZnO layer to get a film about 85 nm thickness. Finally, MoO_3 and Al layers were evaporated on the top of the active layer. The device area, the overlap section between the ITO and Al electrodes, was about 4 mm^2.

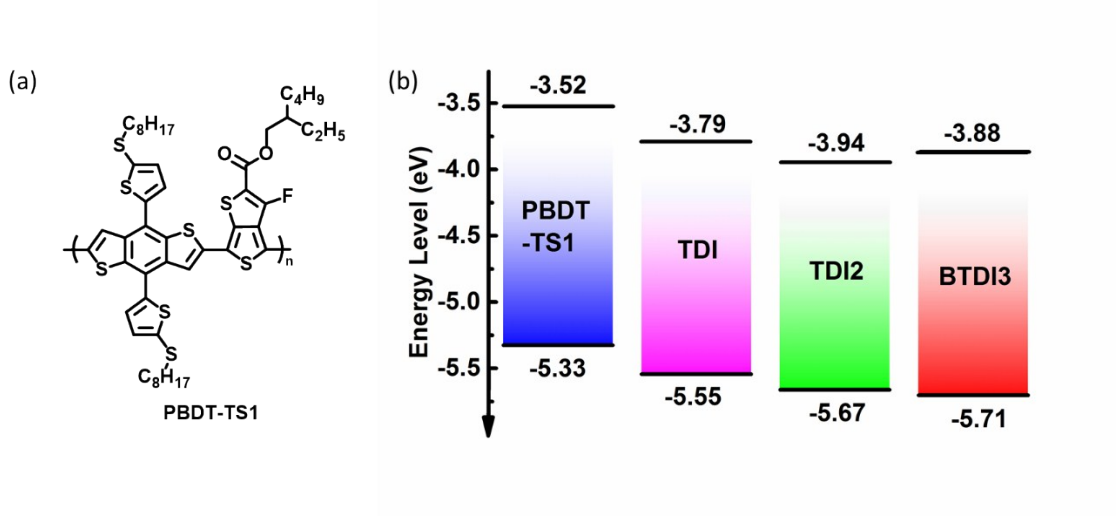

Fig. S6 (a) the chemical structure of PBDT-TS1 and (b) the energy levels of PBDT-TS1, **TDI**, **TDI2** and **BTDI3**.

Table S3 The detailed photovoltaic values of devices based on PBDT-TS1:acceptors tested under illumination of AM 1.5 G (100 mW cm^{-2})

Blends	Ratio	V_{OC} [V]	J_{SC} [mA cm^{-2}]	FF	PCE [%]
PBDT-TS1:**TDI2**	1.5:1	0.64	7.08	0.40	1.80
	1:1	0.66	9.00	0.47	2.79
	1:1.5	0.66	7.03	0.45	2.18
PBDT-TS1:**BTDI3**	1.5:1	0.70	9.07	0.39	2.49
	1:1	0.73	10.77	0.46	3.64
	1:1.5	0.70	10.42	0.39	2.10

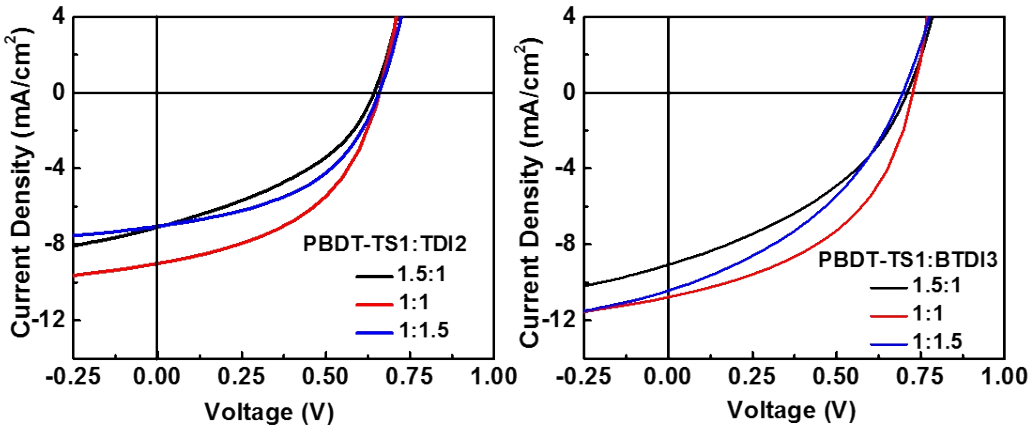

Fig. S7 *J-V* curves of PBDT-TS1: acceptors solar cells by different ratios (w/w).

Table S4 The detailed photovoltaic values of devices based on PBDT-TS1:acceptors tested under illumination of AM 1.5 G (100 mW cm^{-2})

Blends	V_{OC} [V]	J_{SC} [mA cm^{-2}]	FF	PCE [%]
PBDT-TS1:**TDI** 1:1	0.80	8.22	0.41	2.70
	0.79	8.21	0.41	2.66
	0.79	8.16	0.41	2.67
	0.80	8.22	0.42	2.73
	0.79	8.10	0.41	2.60
	0.80	8.29	0.40	2.67
	0.79	8.17	0.40	2.60
	0.79	8.18	0.41	2.64
PBDT-TS1:**TDI2** 1:1	0.66	9.00	0.47	2.79
	0.66	8.86	0.46	2.67
	0.66	8.30	0.49	2.68
	0.66	8.51	0.49	2.72
	0.66	8.51	0.49	2.73
	0.66	8.16	0.50	2.69
	0.66	8.24	0.50	2.69
	0.66	8.28	0.49	2.69
PBDT-TS1:**BTDI3** 1:1	0.72	10.64	0.46	3.55
	0.72	10.82	0.45	3.49
	0.72	10.84	0.46	3.55
	0.72	10.70	0.46	3.54
	0.73	10.77	0.46	3.64
	0.72	10.90	0.46	3.64
	0.72	10.88	0.46	3.64
	0.73	10.58	0.46	3.57

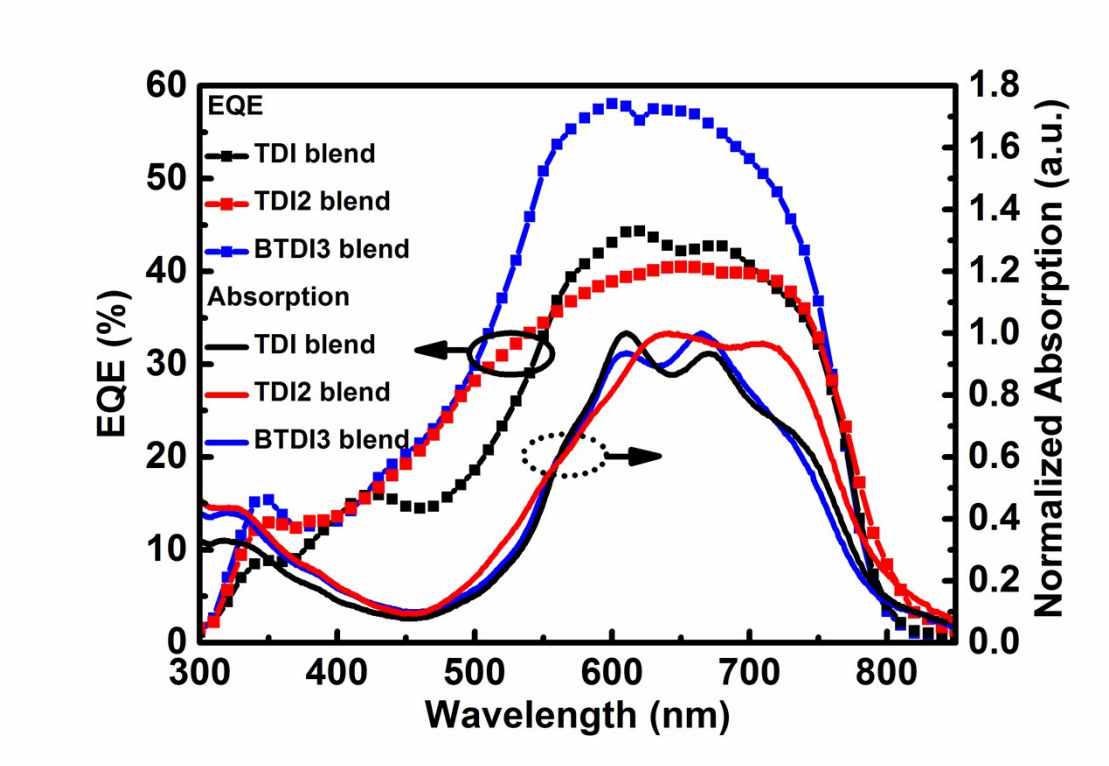

Fig. S8 EQE curves of PBDT-TS1:acceptors based OSCs and UV-vis spectra of blend film.

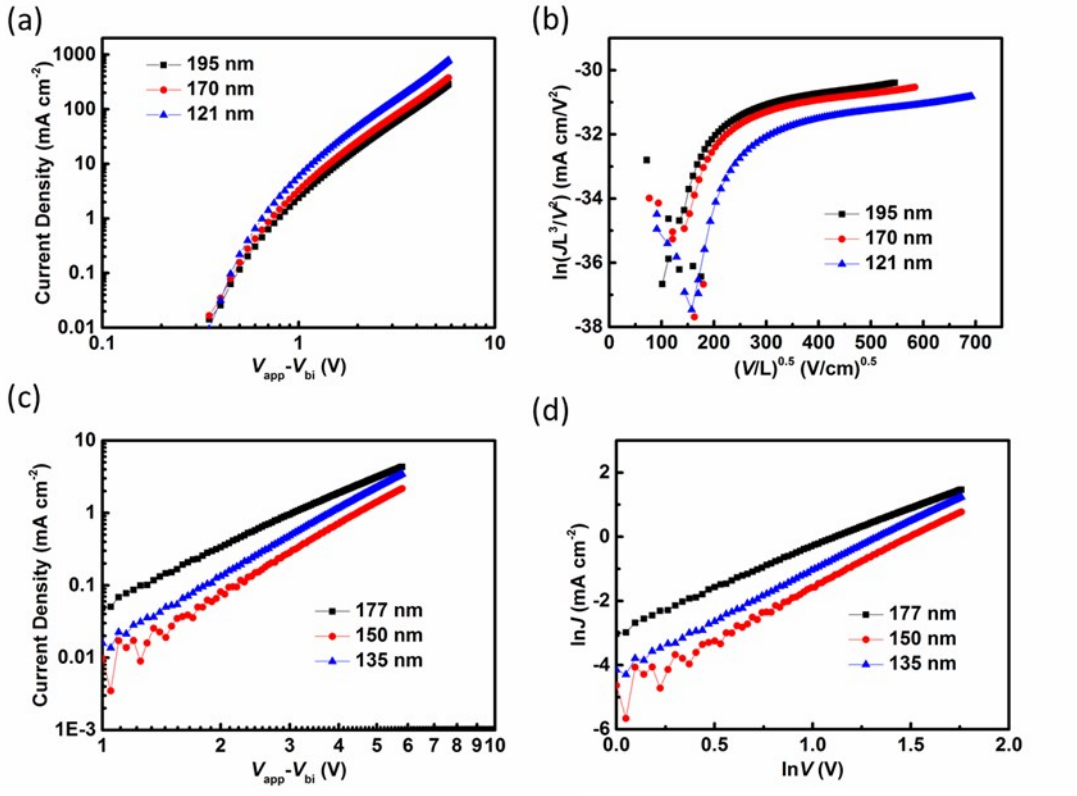

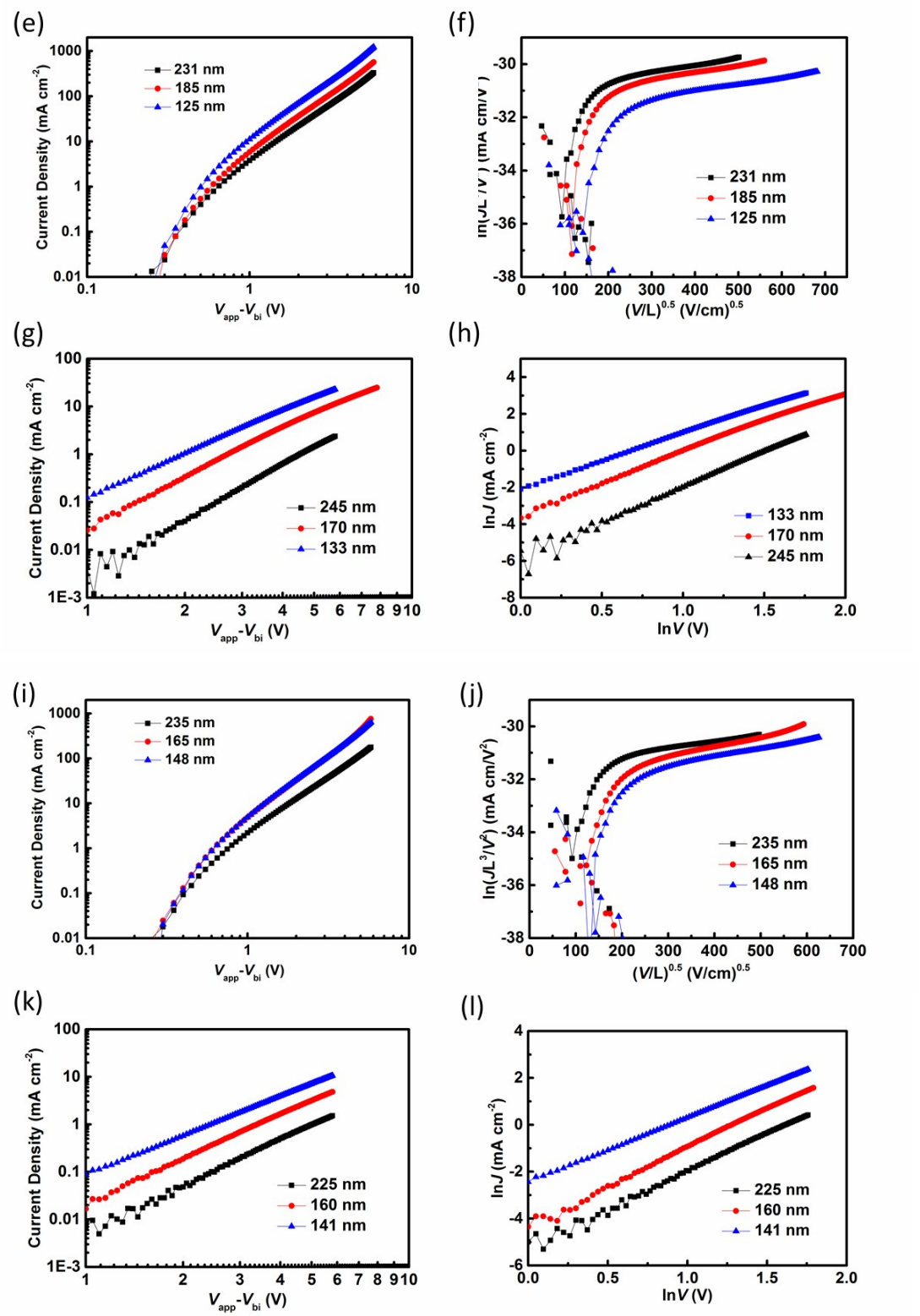

Fig. S9 (a) Plots of J~V (b) plots of ln(Jd^3/V^2) vs $(V/d)^{0.5}$ obtained from the hole-only devices and (c) plots of J~V (d) plots of ln$J$ vs ln$V$ obtained from the electron-only devices for PBDT-TS1:**TDI**. (e) Plots of J~V (f) plots of ln(Jd^3/V^2) vs $(V/d)^{0.5}$ obtained from the hole-only devices and (g) plots of J~V (h) plots of ln$J$ vs ln$V$ obtained from the electron-only devices for PBDT-TS1:**TDI2**. (i) Plots of J~V (j) plots of ln(Jd^3/V^2) vs $(V/d)^{0.5}$ obtained from the hole-only devices and (k) plots of J~V (l) plots of ln$J$ vs ln$V$ obtained from the electron-only devices for PBDT-

TS1:**BTDI3**.

Table S5 Charge transport parameters of the SCLC devices of PDBT-TS1:acceptors blend

Blend	μ_h [cm^{-2} v^{-1} s^{-1}] (thickness [nm])	μ_e [cm^{-2} v^{-1} s^{-1}] (thickness [nm])
PBDT-TS1:**TDI**	6.25×10^{-5} (195)	8.00×10^{-7} (177)
	5.33×10^{-5} (170)	8.13×10^{-8} (150)
	3.20×10^{-5} (121)	9.29×10^{-8} (135)
PBDT-TS1:**TDI2**	1.06×10^{-4} (231)	1.04×10^{-7} (245)
	8.19×10^{-5} (185)	3.51×10^{-7} (170)
	4.03×10^{-5} (125)	7.55×10^{-7} (133)
PBDT-TS1:**BTDI3**	6.64×10^{-5} (235)	1.61×10^{-7} (225)
	3.40×10^{-5} (165)	1.59×10^{-7} (160)
	2.67×10^{-5} (148)	6.22×10^{-7} (141)

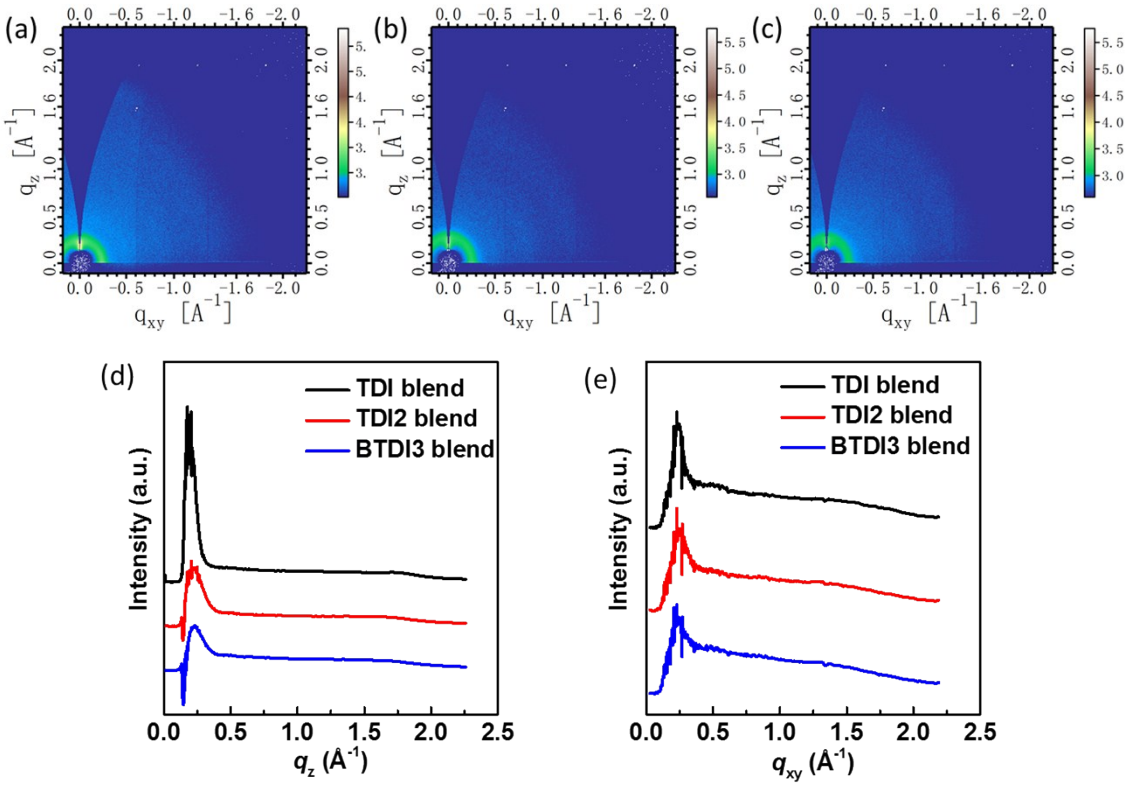

Fig. S10 Two-dimensional GIWAXS patterns of (a) optimal PBDT-TS1:**TDI** blend film, (b) optimal PBDT-TS1:**TDI2** blend film and (c) optimal PBDT-TS1:**BTDI3** blend film. (d) Out-of-plane and (e) in-plane line cuts from 2D GIWAXS patterns.

4. References

(1) W. Li, S. Albrecht, L. Yang, S. Roland, J. R. Tumbleston, T. McAfee, L. Yan, M. A. Kelly, H. Ade, D. Neher and W. You, *J. Am. Chem. Soc.*, 2014, **136**, 15566-15576.

(2) F. Nolde, W. Pisula, S. Müller, C. Kohl and K. Müllen, *Chem. Mater.*, 2006, **18**, 3715-3725.

(3) M. J. Frisch, G. W. Trucks, H. B. Schlegel, G. E. Scuseria, M. A. Robb, J. R. Cheeseman, G. Scalmani, V. Barone, B. Mennucci, G. A. Petersson, H. Nakatsuji, M. Caricato, X. Li, H. P. Hratchian, A. F. Izmaylov, J. Bloino, G. Zheng, J. L. Sonnenberg, M. Hada, M. Ehara, K. Toyota, R. Fukuda, J. Hasegawa, M. Ishida, T. Nakajima, Y. Honda, O. Kitao, H. Nakai, T. Vreven, J. A. Montgomery Jr, J. E. Peralta, F. Ogliaro, M. Bearpark, J. J. Heyd, E. Brothers, K. N. Kudin, V. N. Staroverov, T. Keith, R. Kobayashi, J. Normand, K. Raghavachari, A. Rendell, J. C. Burant, S. S. Iyengar, J. Tomasi, M. Cossi, N. Rega, J. M. Millam, M. Klene, J. E. Knox, J. B. Cross, V. Bakken, C. Adamo, J. Jaramillo, R. Gomperts, R. E. Stratmann, O. Yazyev, A. J. Austin, R. Cammi, C. Pomelli, J. W. Ochterski, R. L. Martin, K. Morokuma, V. G. Zakrzewski, G. A. Voth, P. Salvador, J. J. Dannenberg, S. Dapprich, A. D. Daniels, O. Farkas, J. B. Foresman, J. V. Ortiz, J. Cioslowski and D. J. Fox, *Gaussian 09, Revision D.01*, Gaussian, Inc., Wallingford CT, 2013.

(4) Y. M. Sun, J. H. Seo, C. J. Takacs, J. Seifter and A. J. Heeger, *Adv. Mater*. 2011, **23**, 1679-1683.

^{1}H NMR spectrum of **TDI2** in $CDCl_2$ $CDCl_2$ (373 K)

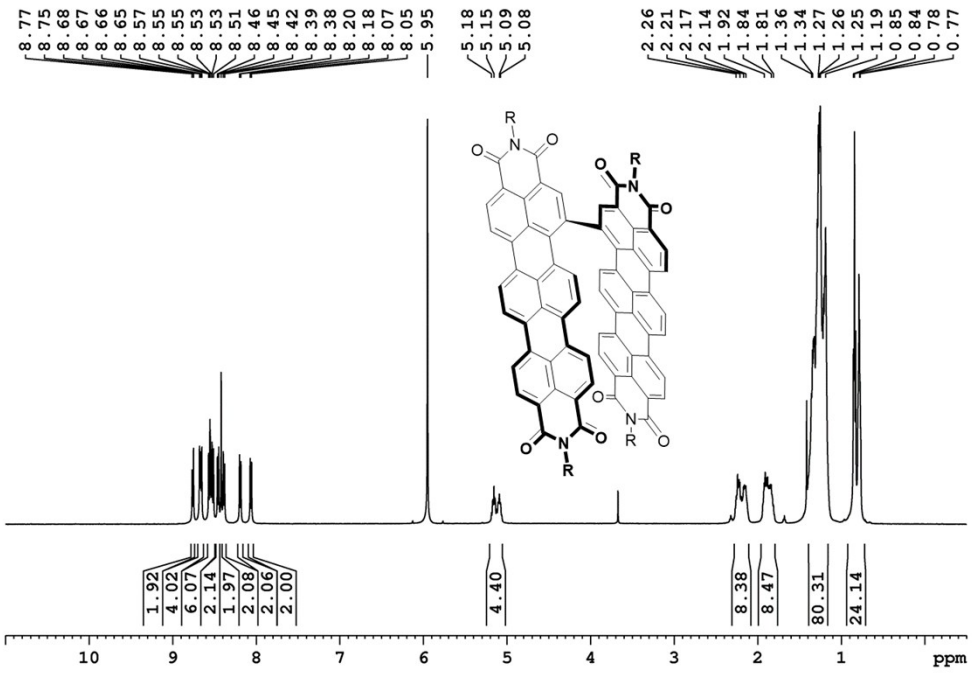

^{13}C NMR spectrum of **TDI2** in $CDCl_2$ $CDCl_2$ (373 K)

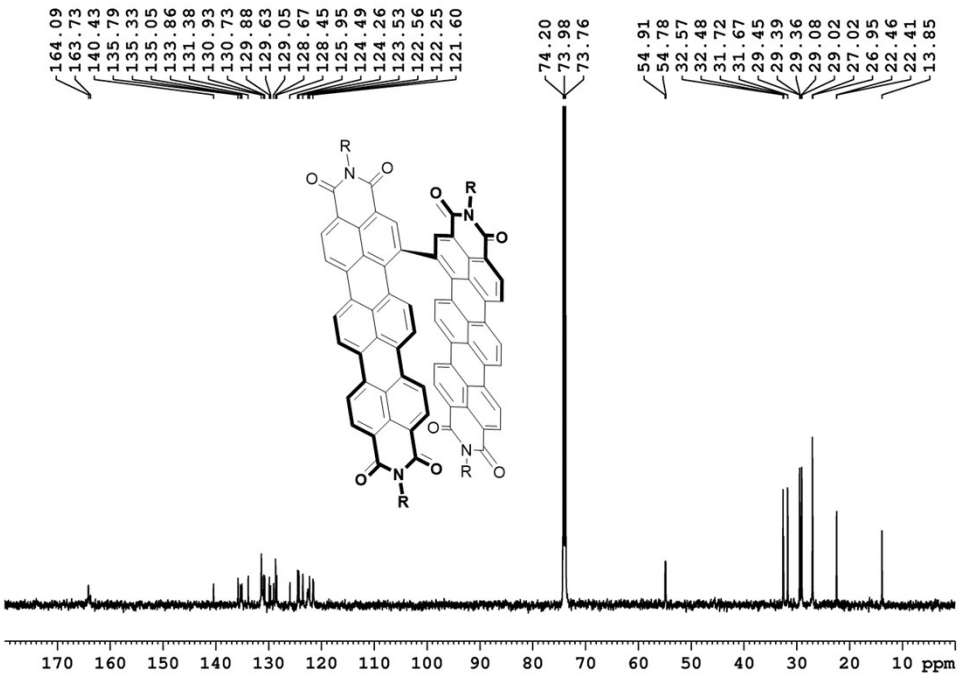

^{1}H NMR spectrum of **TDI2** in $CDCl_2$ $CDCl_2$ (373 K)

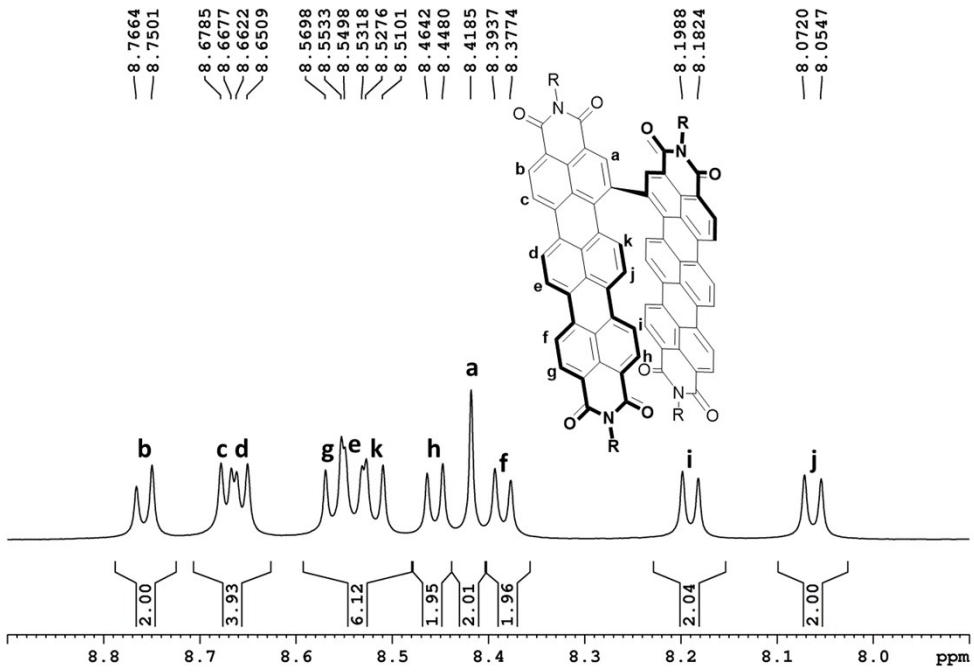

^{1}H-^{1}H Correlation Spectroscopy (^{1}H-^{1}H COSY) of **TDI2** in $CDCl_2$ $CDCl_2$ (373 K)

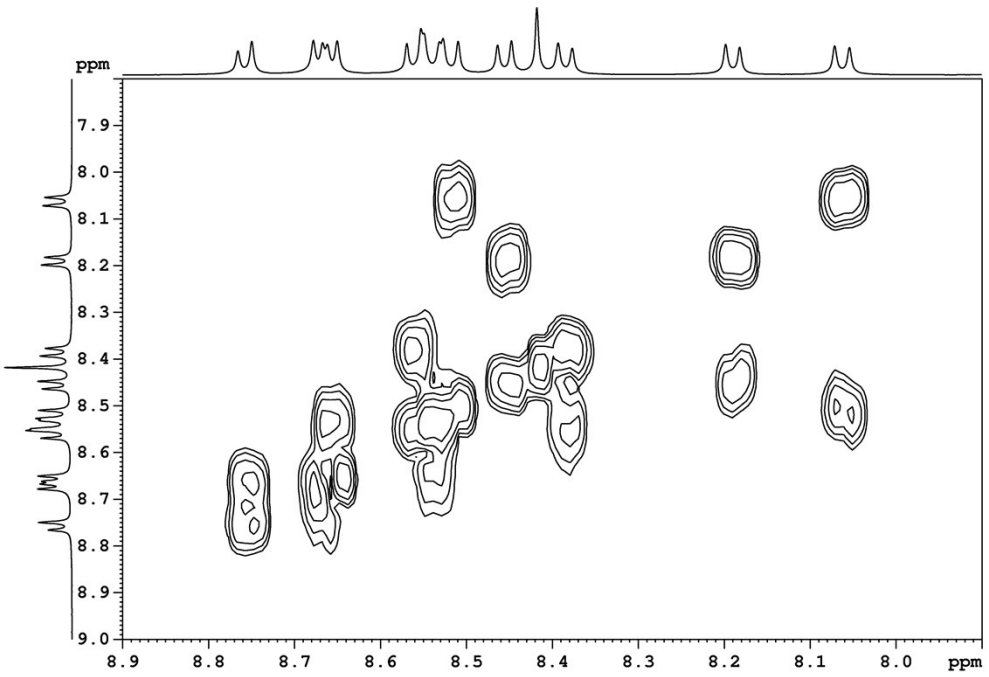

Heteronuclear multiple bond correlation (HMBC) spectrum of **TDI2** in $CDCl_2$ $CDCl_2$ (373 K)

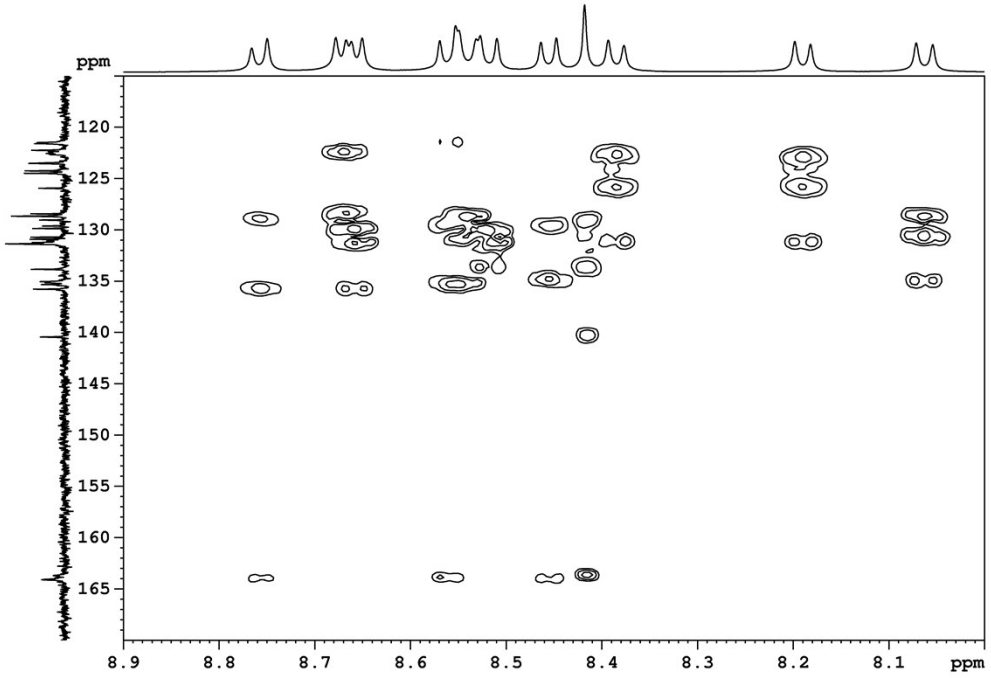

Nuclear Overhauser Effect Spectroscopy (NOESY) of **TDI2** in $CDCl_2$ $CDCl_2$ (373 K)

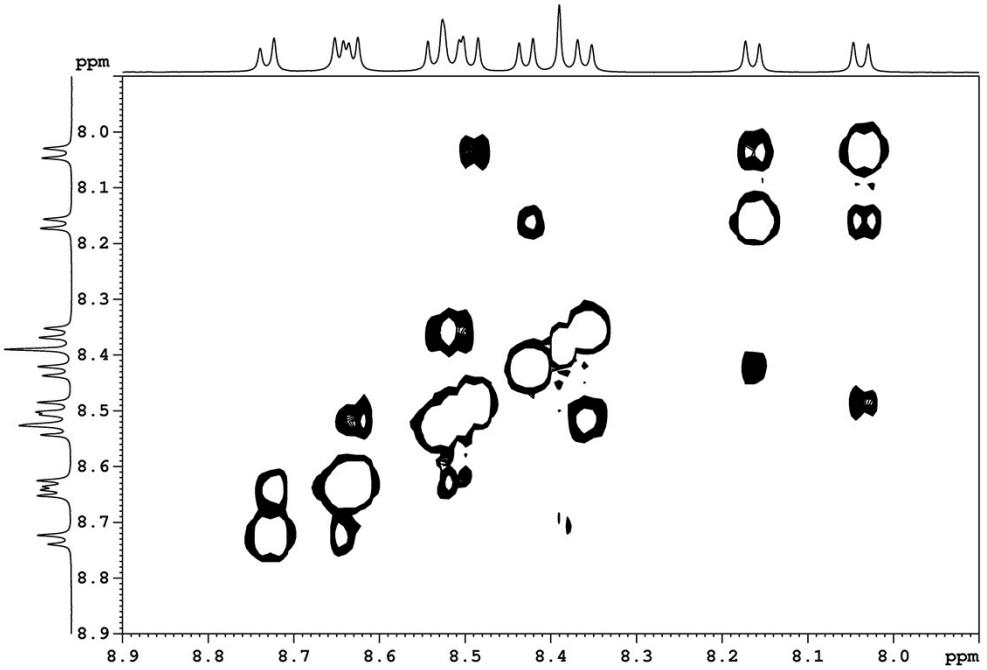

^{1}H NMR spectrum of **BTDI3** in $CDCl_2$ $CDCl_2$ (373 K)

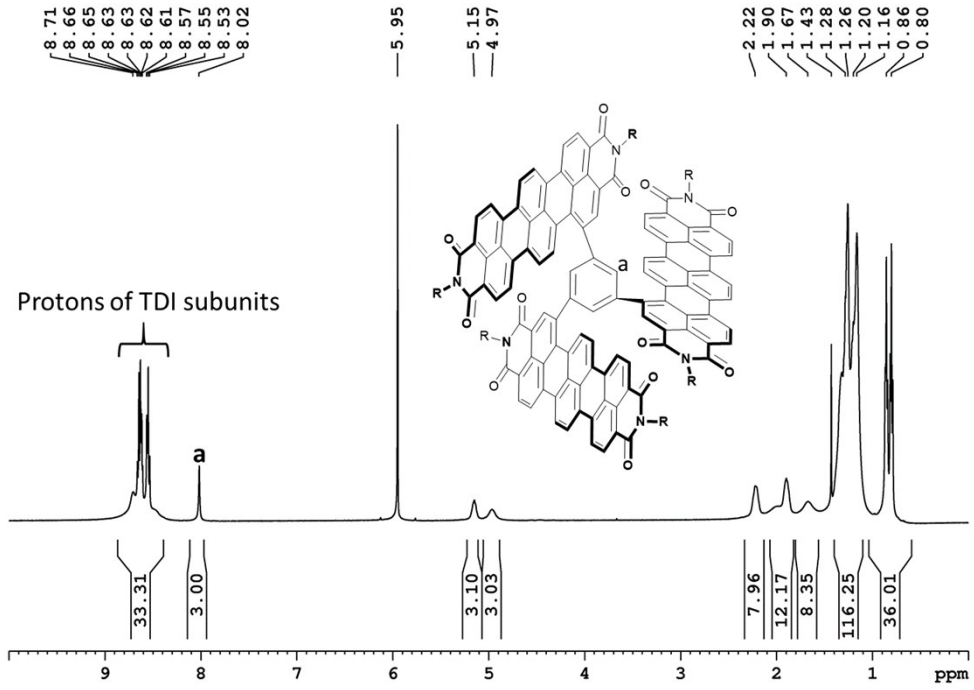

^{13}C NMR spectrum of **BTDI3** in $CDCl_2$ $CDCl_2$ (373 K)

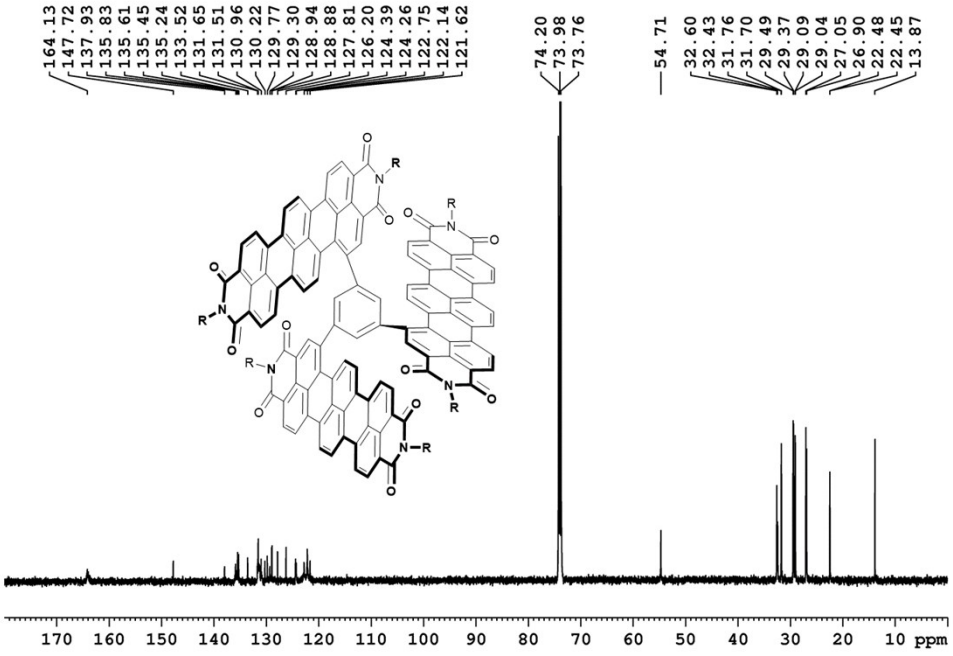

^{1}H NMR spectrum of **1** in $CDCl_2$ $CDCl_2$ (373 K)

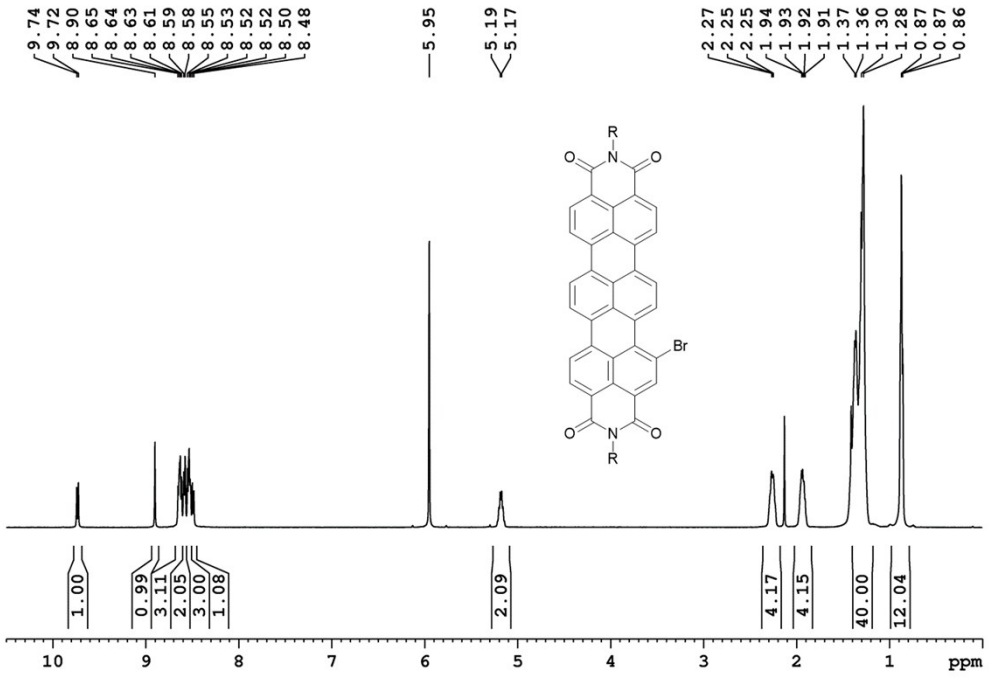

^{13}C NMR spectrum of **1** in $CDCl_2$ $CDCl_2$

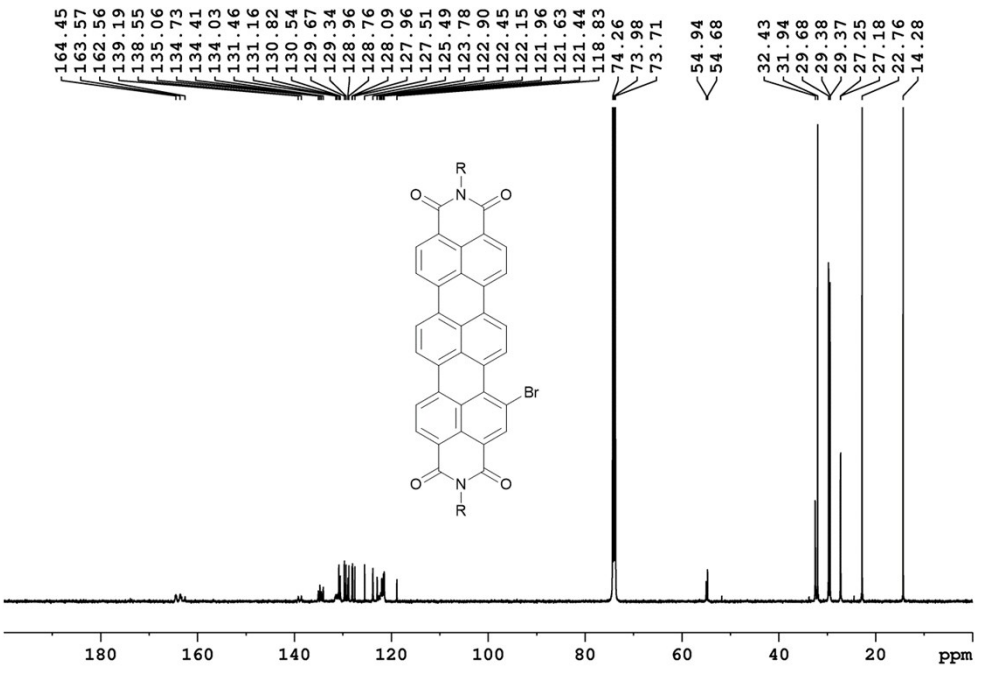

MALDI,F-2,20160530

Analysis Info

Analysis Name	D:\Data\MALDI\2016\0530\F-2_0_D6_000002.d	Acquisition Date	5/30/2016 5:33:39 PM
Method	MALDI_P_100-3000	Operator	
Sample Name		Instrument	solariX
Comment			

Acquisition Parameter

Acquisition Mode	Single MS	Acquired Scans	5	Calibration Date	Mon May 30 05:30:51
Polarity	Negative	No. of Cell Fills	1	Data Acquisition Size	2098152
Broadband Low Mass	202.1 m/z	No. of Laser Shots	10	Data Processing Size	4194304
Broadband High Mass	3600.0 m/z	Laser Power	47.2 lp	Apodization	Sine-Bell Multiplication
Source Accumulation	0.001 sec	Laser Shot Frequency	0.020 sec		
Ion Accumulation Time	0.800 sec				

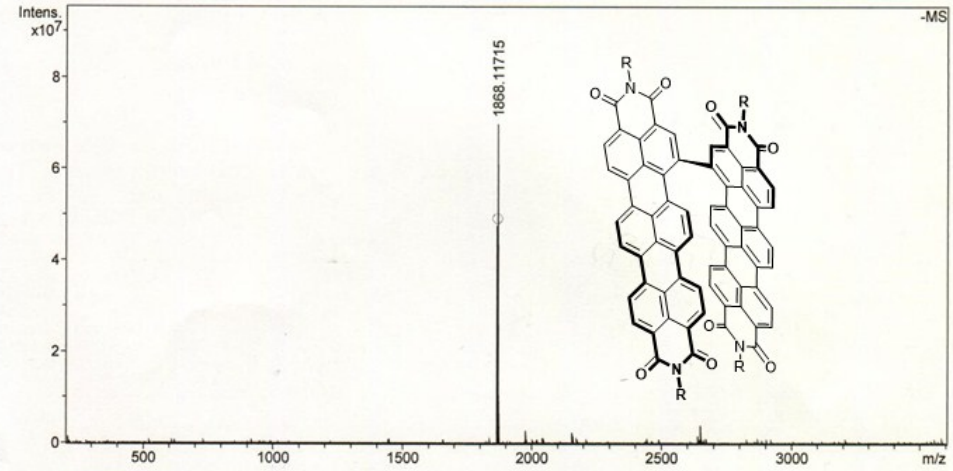

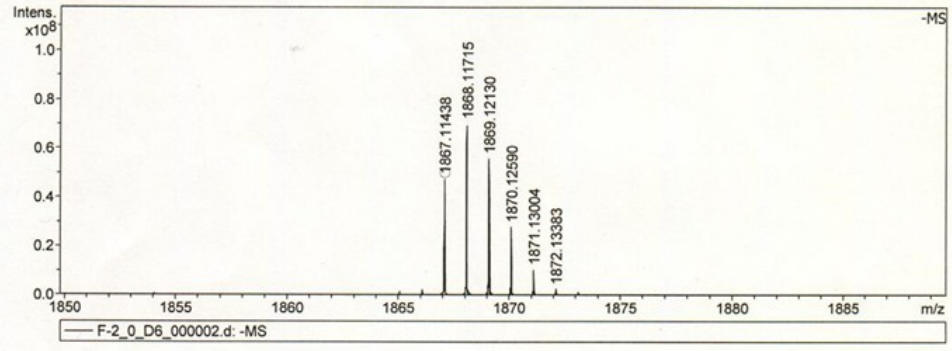

Meas. m/z	#	Ion Formula	Score	m/z	err [ppm]	Mean err [ppm]	mSigma	rdb	e⁻ Conf	N-Rule
1867.114382	1	C128H146N4O8	100.00	1867.114616	-0.1	-0.0	39.7	58.0	odd	ok

MALDI,F-3,20160530

Analysis Info

Analysis Name	D:\Data\MALDI\2016\0530\F-3_0_D7_000020.d	Acquisition Date	5/30/2016 5:55:51 PM
Method	MALDI_P_100-3000	Operator	
Sample Name		Instrument	solariX
Comment			

Acquisition Parameter

Acquisition Mode	Single MS	Acquired Scans	3	Calibration Date	Mon May 30 05:30:51
Polarity	Negative	No. of Cell Fills	1	Data Acquisition Size	2098152
Broadband Low Mass	202.1 m/z	No. of Laser Shots	132	Data Processing Size	4194304
Broadband High Mass	5000.0 m/z	Laser Power	81.8 lp	Apodization	Sine-Bell Multiplication
Source Accumulation	0.001 sec	Laser Shot Frequency	0.020 sec		
Ion Accumulation Time	0.800 sec				

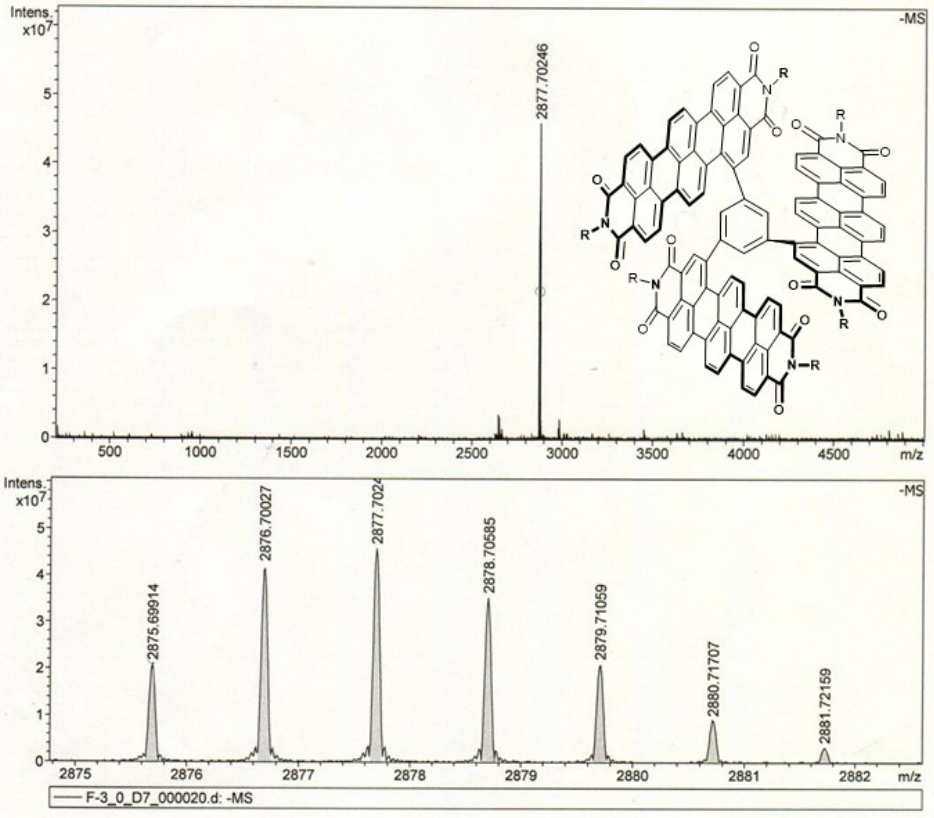

Meas. m/z	#	Ion Formula	Score	m/z	Mean err [ppm]	mSigma	rdb	e⁻ Conf	N-Rule
2875.699137	1	C198H222N6O12	100.00	2875.695125	-0.7	24.6	91.0	odd	ok

MALDI,F-1,20160530

Analysis Info

Analysis Name	D:\Data\MALDI\2016\0530\F-1_0_D5_000001.d	Acquisition Date	5/30/2016 5:27:20 PM
Method	MALDI_P_100-3000	Operator	
Sample Name		Instrument	solariX
Comment			

Acquisition Parameter

Acquisition Mode	Single MS	Acquired Scans	2	Calibration Date	Mon May 30 05:25:06
Polarity	Negative	No. of Cell Fills	1	Data Acquisition Size	2097152
Broadband Low Mass	202.1 m/z	No. of Laser Shots	10	Data Processing Size	4194304
Broadband High Mass	1800.0 m/z	Laser Power	47.6 lp	Apodization	Sine-Bell Multiplication
Source Accumulation	0.001 sec	Laser Shot Frequency	0.020 sec		
Ion Accumulation Time	0.800 sec				

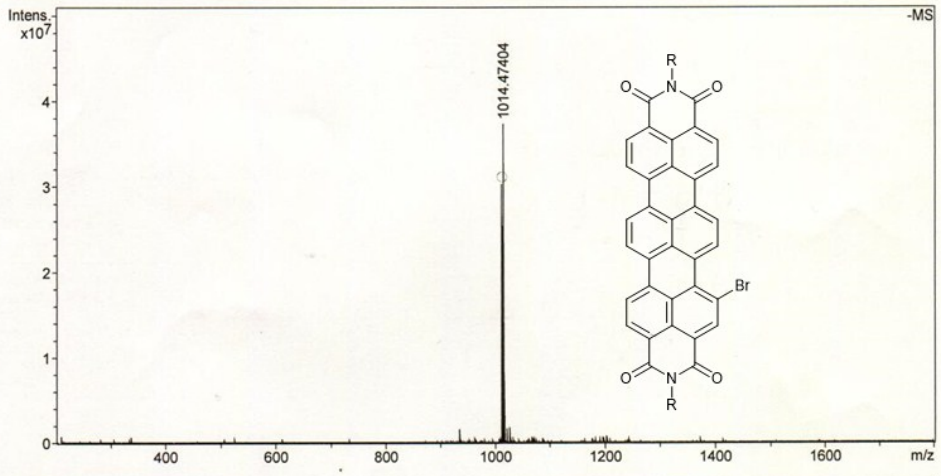

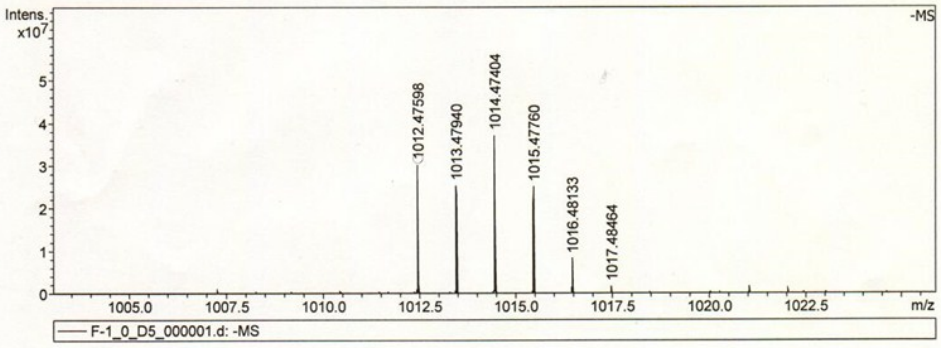

Meas. m/z	#	Ion Formula	Score	m/z	err [ppm]	Mean err [ppm]	mSigma	rdb	e⁻ Conf	N-Rule
1012.475981	1	C64H73BrN2O4	100.00	1012.475920	0.1	0.4	48.2	29.0	odd	ok